On the Summertime Strengthening of the Northern Hemisphere Pacific Sea-Level Pressure Anticyclone

Sumant Nigam and *Steven C. Chan*

Department of Atmospheric and Oceanic Science
University of Maryland, College Park, MD 20742

(Submitted to the *Journal of Climate* on November 8, 2007; revised July 27, 2008)

Corresponding author: Sumant Nigam, 3419 Computer & Space Sciences Bldg.
University of Maryland, College Park, MD 20742-2425; nigam@atmos.umd.edu

Abstract

The study revisits the question posed by Hoskins (1996) on why the Northern Hemisphere Pacific sea-level pressure (SLP) anticyclone is strongest and maximally extended in summer when the Hadley Cell descent in the northern subtropics is the weakest. The paradoxical evolution is revisited because anticyclone build-up to the majestic summer structure is gradual, spread evenly over the preceding 4-6 months, and not just confined to the monsoon-onset period; interesting, as monsoons are posited to be the cause of the summer vigor of the anticyclone.

Anticyclone build-up is moreover found focused in the extratropics; not subtropics, where SLP seasonality is shown to be much weaker; generating a related paradox in context of Hadley Cell's striking seasonality. Showing this seasonality to arise from, and thus represent, remarkable descent variations in the Asian monsoon sector, but not over the central-eastern ocean basins, leads to paradox resolution.

Evolution of other prominent anticyclones is analyzed to critique development mechanisms: Azores High evolves like the Pacific one, but without a monsoon to its immediate west. Mascarene High evolves differently, peaking in austral winter. Monsoons are not implicated in both cases.

Diagnostic modeling of seasonal circulation *development* in the Pacific sector concludes this inquiry. Of the three forcing regions examined, Pacific midlatitudes is found most influential, accounting for over two-thirds of the winter-to-summer SLP development in the extratropics (6-8 hPa), with the bulk coming from the abatement of winter stormtrack heating and transients. The Asian monsoon contribution (2-3 hPa) is dominant in the Pacific (and Atlantic) subtropics.

The modeling results resonate with observational findings, and attest to the demise of winter stormtracks as the principal cause of the summer vigor of the Pacific anticyclone.

1. Introduction

The subtropical sea-level pressure anticyclones – majestic semi-permanent features over northern and southern oceans – are an integral element of the atmospheric general circulation: Their clockwise (in the Northern Hemisphere) near-surface flow connects the Tropical trade wind regime with the midlatitude westerly belt, influencing both. Thermodynamically, the anticyclones reside between the intense convection zones in the deep Tropics and the midlatitude stormtracks which extend from the eastern coasts of the continents to the mid basins, especially in winter. The Northern Hemisphere anticyclones extend well into the midlatitudes in summer, when they occupy close to 50% of the Western Hemisphere surface.[1]

The expansive anticyclones apparently contributed to the naming of the Pacific Ocean and the circumnavigation of the Earth. Sailing under Spanish flag, Ferdinand Magellan entered the South Pacific on November 28, 1521 in his quest to find a westward route to the Spice Islands.[2] Interestingly, Magellan's entry was at a time of the year when regional sea-level pressure is at its seasonal peak (see Fig. 7). As high pressure is synonymous with fair weather, Magellan found calm seas in the initial leg of his Pacific voyage which took him northwestward across the expansive subtropical anticyclone in the southeastern basin[3] – in contrast with stormy conditions encountered in his earlier transit through southwestern Atlantic and the Straits of Tierra del Fuego. The seasonal timing and track of Magellan's pioneering voyage thus presented him with a striking contrast in sea states, leading to his naming of *Mare del Zur* (the South Sea, as Pacific

[1] The 'subtropical' reference of the anticyclones is at some odds with respect to their summer structure, which exhibits robust amplitude in the midlatitudes.

[2] Magellan had earlier visited India in 1505 under Portuguese command taking the eastward route through the Cape of God Hope; and then again in 1508, taking part in battles along the Malabar Coast which lead to Portuguese supremacy over the Indian Ocean. Maritime and economic rivalry lead the Spanish to seek a westward route to the Spice Islands, using Magellan's proven navigational skills.

[3] Antonio Pigafetta accompanied Magellan and survived the circumnavigation to write an account. The open sea they crossed, he wrote, "was well named Pacific, for during this same time we met with no storm." (Peterson 2005).

was called then) as *Mare Pacificum* (Peterson 2005).

The canonical explanation for the existence of the subtropical anticyclones, or at least of the surface high-pressure belt in the subtropics, is the descent in the poleward branch of the meridionally overturning Hadley Cell. That this belt should consists of separate anticyclones and intervening cols (a relative low pressure region), rather than uniform high pressure, was first emphasized by Bergeron (1930) in context of air mass and frontal development. Bjerknes (1935) argued for such a belt structure from stability considerations, and discussed the organization of ascending and descending regions.[4] The subtropical descent is, of course, associated with deserts, both continental and oceanic, and provides unique and critical pathways for radiative cooling of the Tropics ("radiator fins", Pierrehumbert 1994).

The subtropical anticyclones interact with the underlying oceans as well, and not just by suppressing precipitation along their eastern/southeastern flanks (i.e., through salinity impacts): The clockwise circulation over the northern Pacific, for instance, influences the gyre-scale circulation through the wind stress curl, and SSTs along the California Coast from coastal upwelling. The colder SSTs and resulting near-surface coolness coupled with the warming of the lower troposphere from adiabatic descent leads to static stability enhancement (e.g., trade inversion), and in turn, extensive low-level cloudiness with significant radiative impacts in the very regions of suppressed precipitation!

Following Bjerknes' analysis, several hypotheses have been put forward to account for the subtropical anticyclones, including monsoon heating to the east and the west of the anticyclones. The role of eastward heating was noted in a seminal paper by Hoskins (1996; the 1995 Bernhard

[4] See Chapter III (*Production and Transformation of Air Masses*) in Petterssen's 1940 book titled *Weather Analysis and Forecasting* for a brief English language discussion of these papers.

Haurwitz Memorial Lecture of the American Meteorological Society), who discussed the forcing of anticyclones in context of large seasonal fluctuations in their strength and expanse. Hoskins argued that latent heat released over the neighboring land masses to the east during the summer advance of the continental monsoon into the subtropics generates a Rossby wave response to the northwest of monsoon heating, with the related descent (and orographic interaction) contributing to anticyclone development, especially in the eastern basin.

A strong case for both eastward and westward monsoon heating in forcing the NH summer anticyclones, especially the one in the Pacific, was made by Rodwell and Hoskins (2001) from modeling the response of observationally constrained diabatic heating (diagnosed residually from ERA-15 reanalysis) through initial-value integrations of a nonlinear, primitive equation model. Ting (1994) had recognized the importance of both heatings, especially, the Indian monsoon heating in anticyclone forcing earlier (see her Fig. 13), albeit in the more general context of diagnostic modeling of the summertime circulation.[5] The importance of westward heating was also shown by Chen et al. (2001), from quasi-geostrophic modeling analysis. Seager et al. (2003) suggested that the summer strength of the Pacific anticyclone is, secondarily, due to local air-sea interaction at the far ends of the basin, which lead to zonal SST variations, and, in turn, modulation of the heating distribution; which is consequential.

The influence of local diabatic heating on the summer anticyclone was also assessed by Rodwell and Hoskins (2001), who found low-level diabatic cooling in the northeastern Pacific to be influential. Since this cooling is, in part, due to the longwave emission from stratus cloud tops, it depends on the large-scale adiabatic descent over the anticyclone's eastern/southeastern flank

[5] Ting analyzed the summertime circulation generated by the Geophysical Fluid Dynamics Laboratory's (GFDL) GCM, using a steady-state, linear, primitive equation model. The assessment of the influence of various monsoon heatings is insightful, but some caution is in order given the significantly stronger summertime stationary waves in this GCM; by a factor of ~2 in the lower troposphere (see Figs. 1b and 2b in Ting's paper). This is consistent with the stronger diabatic heating in the GCM; for example, heating in the Indian and western Pacific sector is larger by a factor of 1.5-2.0 vis-à-vis the observationally constrained heating estimate (cf. Fig. 2 in Rodwell and Hoskins 2001).

for sustenance. As such, its influence, while considerable, is of a feedback rather than causative nature.[6]

It is noteworthy that the above cited studies focus on modeling the summer circulation; not circulation development, the pertinent modeling target in context of the summer peaking of anticyclone's strength and expanse. The origin of the winter-to-summer change in circulation features, for instance, depends as much on the winter forcing as the summer one, especially, in case of gradual development. Modeling either circulation should, nonetheless, provide some insights into the origin of circulation evolution, as the above cited studies sought to do from modeling of the summertime flow.

The monsoon heating – intrinsically seasonal – could well account for the summer vigor of the anticyclones. The continental heating to the east and west of the Pacific anticyclone, for example, is undoubtedly influential in the above modeling studies. The modeled monsoon influence (especially, Asian monsoon's) however extends over large parts of the tropical and subtropical Pacific (e.g., central/eastern basin) where seasonal sea-level pressure development is weak in nature (a section 3 finding). The monsoons may thus not be the only significant influence in the region or their impact could replace another that abates from winter-to-summer. Observational analysis, described in section 3, moreover shows the largest winter-to-summer Pacific sea-level pressure change to occur in the middle and high latitude basin.[7] Together, these observational features suggest that the reasons for the summer robustness of the NH anticyclone may not all be known.

[6] A similar feedback from stratus cloud-top cooling fosters the annual warm-to-cold SST transition in the eastern tropical Pacific in modeling analysis of Nigam (1997), who argued that dynamic feedback of cloud-top longwave cooling in coastal upwelling regions is more rapid than the thermodynamic feedback from stratus shading.

[7] Eastern Hemisphere monsoons are found influential in this region too in the cited modeling studies but the influence was generated from an overly extended diabatic heat source in most cases: up to 150E-170W to the east and 60N; making separation of local and remote effects difficult.

This observationally rooted study revisits the question posed by Hoskins (1996, and Ed Sarachik) on why the NH anticyclones are strongest and maximally extended in summer when the Hadley Cell descent in northern latitudes is the weakest? It begins with the examination of seasonal sea-level pressure development in the Pacific basin. The characterization of annual variability, especially, the finding of incremental build-up of the anticyclone during spring and summer months raises the spectre of incomplete understanding; necessitating a revisit of the anticyclone development question.

The study seeks to critique the mechanisms advanced for the impressive waxing and waning of the NH anticyclones, especially, the Pacific one from both observational and diagnostic modeling analyses. Intercomparison of seasonal sea-level pressure (SLP) variability in the Pacific and Atlantic basins (section 3); analysis of monthly evolution of upper-tropospheric descent in the northern subtropics (section 4); examination of seasonal structure of the 200 hPa divergent circulation (section 5); and intercomparion of annual SLP variability in the Northern and Southern Hemispheres (section 6) contribute to the observational assessment. The modeling analysis begins in section 7 which describes the diagnostic model, its forcing data sets, and its performance. The dynamical diagnosis of winter-to-summer SLP development, especially the contribution of regional forcing onsets/abatements is presented in section 8. Concluding remarks follow in section 9.

2. Data sets

The European Centre for Medium-Range Weather Forecasts (ECMWF) global reanalysis data provides the necessary atmospheric variables for the present analysis. The ECMWF 40-year global reanalysis (ERA-40; Uppala et al 2005) spans September 1957-August 2002 and is locally available on a 2.5° grid and 23 levels in the vertical. The seasonal evolution is analyzed using the

calendar month climatology for the satellite era (1979-2001).

Monthly precipitation data came from the Climate Prediction Center (CPC) Merged Analysis of Precipitation (CMAP; Xie and Arkin 1997). The CMAP precipitation is also available on a 2.5° grid, and the observation-only CMAP product (CMAP-2) was used.

3. Seasonal variability of Pacific sea-level pressure

The monthly distribution of SLP and precipitation is shown in Fig. 1 for the first half of the calendar year. The most remarkable SLP change is the winter-to-summer abatement and northward retreat of the Aleutian Low and its replacement by high pressure, especially in the central and eastern basin; resulting in a majestic anticyclone in July. The synchronicity of these changes is noteworthy. At its peak, the anticyclone is centered in the 35-40N band and extends over most of the extratropical basin. In contrast, the anticyclone is quite weak in January when it is confined to the far eastern basin. The January-to-July change in core pressure is ~ 6 hPa, but substantially larger SLP change occurs in the northern basin (as shown later).

The concurrent seasonal change in precipitation, which reflect vertically averaged latent heating, are depicted on the same panels for context. Winter precipitation occurs along the southern flank of the Aleutian Low which forms the axis of the jet and winter storm tracks, and along its eastern/southeastern flank where the large-scale vorticity balance – the Sverdrup balance – implies low-level convergence, and thus ascending motion and rainfall: the winter rainy season in the Pacific Northwest (see Nigam and Ruiz-Barradas 2006 for more discussion, including relative contribution of the transient moisture fluxes to winter rainfall). The Aleutian Low is, of course, itself forced in good measure by the stormtrack diabatic heating and transients (cf. Fig. 9b in Hoskins and Valdes 1990, and Fig. 11e in this paper). With the onset of spring and summer, the Aleutian Low retreats northward and related precipitation impacts diminish,

vanishing altogether by July when the US West Coast is under the influence of descending motions associated with the eastern flank of the anticyclone; California's "Mediterranean" summer climate. Further equatorward, the Asian and American monsoons and the Inter-Tropical Convergence Zone (ITCZ) are fully developed by July; note the double ITCZ in March.

The location and spatial extent of the SLP anticyclone is tracked in Fig. 2 by monitoring the movement of the 1020 hPa SLP contour in alternate months, beginning with January ('1'). The tracking of curves labeled 1 through 7 indicates that anticyclone development during spring and summer primarily involves northward advance of the high pressure region; the westward advance occurring earlier (late winter). The most striking feature however is the little change in the subtropical basin, as evident from the overlap of the March-to-July (3, 5, and 7) isobars.

The case for the absence of significant seasonal SLP-change in the tropical and subtropical basin is directly made in Fig. 3, which displays the SLP change over two month periods; along with the Tropic of Cancer for positional reference. The largest two-month change in the build-up phase is between January and March (~8 hPa in the top panel) when SLP increases over the extratropical Pacific in the Aleutian Low longitudes (i.e., the central basin; cf. Fig. 1a). Meridionally, this SLP change is in quadrature with the Aleutian Low, so that the Low is confined to the northern basin in March. It is noteworthy that the largest seasonal increase in SLP in the tropics/subtropics (e.g., the 15-30N belt) – up to 4 hPa – occurs in this period. The subsequent March-May change (panel *b*) is focused in the midlatitudes but with some preference for the western basin. The following May-July SLP change is more like the January-March change in the midlatitudes but with the Tropics and subtropics exhibiting 1-2 hPa reduction in SLP! The reduction is moreover concentrated in the western and eastern basin, adjacent to the warm continents; and consistent with the reach of the continental monsoons, especially, the

Asian one to the west.

The lower panels of Fig. 3 mirror the development portrayed in upper panels, except for the sign. Cyclonic development begins in early autumn and proceeds with increasing vigor with the advent of winter. This development is also focused in the northern midlatitude basin but for the presence of continental influences in the subtropics in autumn which mirror the springtime change. Seasonal SLP variability in the Pacific is evidently annual in nature – in contrast with seasonal variability in the tropical-subtropical Atlantic (not shown) which is more semi-annual.[8]

The May-to-July SLP reduction, albeit modest but occurring in the monsoon onset period, is seemingly at odds with the modeling analyses indicating a role for Asian monsoon heating in anticyclone development. These studies show that Asian monsoon heating leads to positive (and not negative) SLP response in the Pacific tropics and extratropics (Fig. 12b in Ting 1994; Fig. 9a in Chen at al. 2001)[9]. Ting's analysis (Fig. 12) also shows the low-level response over the Pacific to be both augmented and offset by heating in other sectors. The possibility that monsoon heating's influence over the Pacific is offset by other thermal and/or mechanical forcing in nature was raised in the introduction section.

The seasonal cycle of Pacific SLP is compactly shown in context of its annual-mean distribution in Fig. 4 (top panel). The amplitude and phase of the annual harmonic is denoted by the length and direction of the plotted arrows; arrows pointing due north (locally) indicate a summer maximum and a winter minimum. The annual-mean distribution consists of a High in

[8] The Atlantic sector (100-60W) is more responsive to the twice-yearly overhead position of the Sun at the Tropics of Cancer because of the presence of land in this sector (eastern Mexico, Florida and Cuba, among others); with low SLP following the equinoxes within a month, at monthly resolution.

[9] Rodwell and Hoskins' (2001) modeling analysis does not show the low-level streamfunction (or SLP) forced by Asian monsoon heating alone. The closest is the response of orography and Asian monsoon heating (Fig. 8b), with positive SLP in the Pacific tropics and extratropics in July. Their Asian heating box (10S-60N; 60-150E) also seems too inclusive as the Western North Pacific monsoon is within the box.

the eastern subtropical basin and a Low in the northern basin, reflecting some persistence of the summer and winter features in these regions, respectively.

More striking though is the distribution of annual variability: Weaker than 1 hPa in amplitude (the vector plotting threshold) in the entire tropics and subtropics, excluding the far western and eastern coastal sectors where the influence of continental monsoons is manifest, with lower SLP in July. Robust annual variability is however found in the middle and high latitudes, with the amplitudes being particularly large northward of 35N in the central and eastern basin. The structure of annual SLP variability over the Pacific basin raises interesting questions:

- Why is seasonal SLP variability in the Pacific subtropics so weak despite the significant winter-to-summer variation of Hadley Cell descent in these latitudes? The question is similar to the one posed by Hoskins (1996), except that it is the weak seasonal signal in the tropics/subtropics (cf. Figs. 2-4) rather than perceptions of a counterintuitive one (cf. Hoskins 1996) that is enigmatic.
- How significant and extensive is the influence of continental monsoons on Pacific SLP, especially in the northern basin which exhibits striking, albeit gradual, development?

Prior to seeking answers from a modeling analysis (section 7), clues are sought in the structure of seasonal SLP variability in the Atlantic basin, which doesn't have an Asian monsoon equivalent to its west. The annual cycle of Atlantic SLP is displayed in the lower panel of Fig. 4 using the same scale and format, as earlier, to facilitate intercomparison. The annual-mean field consists of a basin-wide anticyclone, called the Azores High (or Bermuda High), which exhibits weak annual variability except at its northern flank.

Annual SLP variability in the Atlantic is, evidently, largest in the northern basin, much as in

the Pacific; and quite weak in the tropical and subtropical latitudes of the interior basin, as also in the Pacific. The similarity continues in near-coastal regions where continental influences (and summer low pressures) are manifest in both basins. The correspondence of annual SLP variations in the two basins is striking and remarkable considering that one of them has a powerful monsoon system to its west. The similarity suggests that having a monsoon to the west of the anticyclone may be inconsequential or else the global reach of the Asian summer monsoon.

4. Evolution of upper-tropospheric descent

The striking winter-to-summer variation of the Hadley Cell along with perceptions that such variability typifies seasonal changes across most longitudes is at the core of the conundrum implicit in the first of the above questions. Recent analysis of Dima and Wallace (2003) however shows Hadley Cell's seasonality to be linked with the monsoons, i.e., with *regional* circulations forced by summer heating of the continents; in agreement with early views of Hadley Cell seasonality (Newell et al. 1972). The analysis shows that Hadley Cell's seasonality is reflective of regionally concentrated rather than longitudinally wide-spread seasonal changes in divergent circulation; correcting flawed perceptions to the contrary.

The Dima-Wallace analysis is supplemented in this section by displaying the monthly evolution of upper-level descent across all longitudes in the northern subtropics, including oceanic mid-basins where SLP variability was found to be weak (Figs. 2-4). The negative of the 300 hPa pressure vertical velocity ($-\omega_{300}$) is plotted in the 15N-25N band in Fig. 5, with the zonal-mean plotted in the adjacent right panel.[10] The band was chosen to fully include the winter and summer descent regions over the Pacific and Atlantic basins (cf. Fig. 6).

[10] An upper rather than mid-troposphere level was chosen to avoid the below-ground interpolated values, given the presence of high mountains in the northern subtropics.

The descent is strongest in winter across most longitudes, much as expected; with the zonal-mean change (right panel) being representative of winter development in most longitudes. The descent varies little between winter and spring, continuing unabated until late spring in some sectors (e.g., Sahara desert, and the western-central Pacific and mid-Atlantic basins); that is, during the period of Hadley Cell's transformation from a single-cell winter structure to a more evenly balanced two-cell equinoctial configuration. The zonal-mean descent is clearly impacted by the development of the Asian and North American monsoons in late spring. The monsoon impact in summer is, of course, overwhelming, with strong, deep ascent manifest not only in the Asian and American longitudes but also in the zonal-mean; leading to northward extension of the rising branch (e.g., ERA-40 Atlas, Kallberg et al. 2005), and thus, narrowing of the summer cell. Further to the north (e.g., 25–30N), monsoon ascent leads to reduction in zonal-mean subsidence, i.e., to cell-weakening. Monsoons are thus integral to Hadley Cell's seasonality, in both strength and structure; in accord with Dima and Wallace (2003).

In context of anticyclone development, Fig. 5 shows the upper-level descent over oceanic basins to be weaker in summer, reflecting some influence of the Asian and Western North Pacific monsoons. The May-July SLP change in the 15-25N latitude band is weakly negative (cf. Fig. 3c), consistent with descent evolution. The conundrum is resolved by first noting that Hadley Cell's striking seasonality is not reflective of seasonal changes across most longitudes, as illustrated by the weak seasonality of descent over the Pacific and Atlantic mid-basins. Positive SLP development in summer is, moreover, focused well to the north of this band, closer to 45N (cf. Figs. 2-4). As such, there is no discord between weaker subtropical descent and positive SLP development in the midlatitude basin. The disaccord suggested in Hoskins (1996) was based on perceptions of positive SLP development in the subtropics; a development that really occurs in the midlatitude basin, as shown here.

5. Monsoon's influence on Pacific basin descent

The influence of Asian monsoon on the far-field circulation is difficult to characterize from observational analysis, given the concurrent seasonal evolution of other climate features, e.g., ITCZ development in the central/eastern equatorial Pacific. The far-field influence consists of both rotational and divergent components, with identification of the former being challenging, observationally, in view of Rossby wave propagation. The presence of multiple wave sources and refractive index variations (e.g., Karoly and Hoskins 1982, Nigam and Lindzen 1989) can often be confounding. Not surprisingly, the monsoon influence is generally characterized using dynamical models (e.g., Ting 1994, Rodwell and Hoskins 2001).

The monsoon's influence on upper-level divergent flow is, conceptually, somewhat easier to identify, given the certainty in where this flow originates – in regions of strong monsoon latent heating. Determination of the flow field however requires knowledge of both origination (divergent outflow) and termination (sinking) points, since the surrounding sinking regions are far from uniformly distributed with respect to the outflow core. The sinking regions, it turns out, are determined both by the divergent outflow structure and its rotational response, and the static stability distribution (e.g., Sardeshmukh 1993), i.e., from complex dynamical and thermodynamical processes, not all of which are presently well understood.

Notwithstanding such difficulties, the 200 hPa divergent flow is tracked from regions of strong monsoon latent heating in Fig. 6, and the monsoon's influence taken to extend, at least, as far as the nearest sinking region. Immediately apparent is the large summer divergent outflow from the Bay of Bengal – the region exhibiting strongest divergence in the Eastern Hemisphere – headed mostly northwestward, westward, and southward. The organization of descent (and ascent) to the northwest bears imprints of Rossby wave propagation, which Rodwell and Hoskins

(1996) emphasized in connecting the Asian summer monsoon with the aridity of western Afghanistan and eastern Iran (the first descent region), and the eastern Mediterranean (the second descent region to the northwest). The bulk of South Asian summer monsoon outflow is however directed southward, to the subtropical Southern Indian Ocean where it leads to the strengthening of the Mascarene High (Krishnamurti and Bhalme 1976). This *regional* meridional overturning is the principal contributor to the austral winter's *zonal-mean* Hadley Cell.

The continental monsoon's influence to the east – the focus here in context of the summer strengthening of the Pacific anticyclone – is comparatively muted in the upper-level descent field, unless one also considers the Western North Pacific monsoon when this influence becomes more appreciable, but still modest. That this monsoon system can be assumed to be independent of the Pacific SLP anticyclone is however not clear for it can be argued that this monsoon owes its existence, in part, to the SLP anticyclone itself (Rodwell and Hoskins 2001). This synergism can contribute to anticyclone development but if the related upper-level descent in Fig. 6 provides any guidance, the Western North Pacific monsoon's influence is modest and confined largely to the tropics, except in the far eastern basin where the subtropics are also, to an extent, influenced. Examination of the 200 hPa divergent circulation indicates the Asian monsoon's influence on upper-level descent over the Pacific to be modest. This, of course, is not a full measure of the monsoon's influence on the Pacific basin, as noted at the beginning of this section. Vorticity dynamics, in particular, vortex stretching in the monsoon latent-heat release regions, elicits a substantial rotational response with bearing on the SLP field – a response, difficult to isolate without the use of models. The related modeling analysis is reported in section 8.

6. Evolution of sea-level pressure in the Southern Hemisphere

The seasonal variability of SLP in the hemisphere having significantly less landmass is examined in this section. Reduced landmass in the sub-polar Southern Hemisphere (SH) leads to weaker stationary waves, and thus, a more axisymmetric circulation. The stormtracks are more zonal as well, especially in summer (e.g., Hoskins and Hodges 2005). The reduced continentality also leads to weaker monsoons. Such differences make SH attractive for testing understanding of the atmospheric general circulation.

The annual variability of SLP in the SH is displayed in Fig. 7. The annual-mean field (contoured) is quite zonal in the high latitudes, unlike in the NH. A weak High in the Weddell Sea sector and a zonally diffuse Low elsewhere is, nonetheless, discernible. The annual-mean SLP also contains three anticyclones in the SH subtropics, one in each ocean basin, with the Indian Ocean one (the Mascarene High) being the strongest (>1022 hPa).

The annual variability of SLP in the SH is quite distinct from the NH, as evident from the distribution and orientation of the annual-harmonic arrows in Fig. 7. The annual variability is primarily focused in the tropical/subtropical latitudes; unlike NH, where high latitudes are the focus region (cf. Fig. 4). This difference leads to strikingly different evolution: An equatorward strengthening/expansion of the SH anticyclones as opposed to poleward development of the NH ones. Phase differences, moreover, lead to different peak-phase timings: austral winter and boreal summer, respectively. What could cause such inter-hemispheric differences in SLP evolutions?

- *Stormtracks*: The SH storm tracks are located in the high latitudes, close to the Antarctic Circle.[11] As such, they are well separated from the subtropical anticyclones, and perhaps, less

[11] The poleward location (~60S) of the SH storm tracks can be seen in the band-pass filtered variance of SLP. Compare, for instance, the NH winter (DJF) distribution (Fig. 3a in Hoskins and Hodges 2002) with the SH winter

influential. This is unlike the NH where storm tracks are mostly in the midlatitudes (40-50N), i.e., in proximity to the SLP anticyclones.

- *Monsoons*: The SH monsoons are weaker, with the monsoon regions located somewhat equatorward; which further reduces their influence (Rodwell and Hoskins 2001). Even so, there is considerable rainfall development over subtropical South America, including Amazonia, from winter (JJA) to summer (DJF). Assuming some monsoon influence on downstream SLP development, one would expect a stronger anticyclone in the subtropical South Atlantic in austral summer (DJF).[12] Observations however indicate the anticyclone to be stronger in austral winter, as is the one in the Indian Ocean.
- *Hadley descent*: Meridional overturning in the Eastern Hemisphere is the principal contributor to the Hadley Cell, including its seasonality (cf. Fig. 6). Descent in the SH tropics/subtropics is strongest in JJA and focused in this sector, as it is related to the Asian/African monsoon outflow. Not surprisingly, this sector's SLP anticyclones are strongest in austral winter.

The evolution of Southern Hemisphere's SLP anticyclones suggests

- Monsoons do not account for the seasonal strengthening of the anticyclones, which peak in austral winter.
- Stormtracks cannot be implicated either given their sub-polar, and thus distant, location relative to the subtropical anticyclones.
- Hadley Cell seasonality can apparently account for the waxing and waning of the SH anticyclones, in accordance with dynamical intuition; quite unlike the case in the NH. Reduced interference from stormtracks is, perhaps, the reason for the manifestation of

(JJA) one (Fig. 3f in Hoskins and Hodges 2005).

[12] A similar dynamical response (e.g., from Sverdrup vorticity balance) is expected in the SH despite the negative Coriolis parameter, for it appears in both the vortex stretching term and the geostrophic relationship.

this intuitive link in SH circulation.

7. Diagnostic model, forcing data sets, and performance

A modeling analysis of Pacific circulation and SLP is undertaken using the ERA-40 data set, with the goal of identifying the regional forcing that leads to the development of key SLP features, including winter-to-summer strengthening/expansion of the anticyclone. This section describes the diagnostic model along with its forcing data sets, and the model's performance.

Diagnostic model

The steady linear primitive equation model solves the σ-coordinate (=p/p_s) equations. The equations are linearized about a zonally symmetric basic state, and the model solves for the eddy component (i.e., deviation from the zonal average) of the circulation. The linearized equations are given in Held et al. (1989) and modifications to represent vertical diffusion processes in the planetary boundary layer in Nigam (1997). Diffusion coefficients vary in the vertical, decreasing rapidly above 850 hPa; all as $30[1+tanh\{10\pi(\sigma-0.85)\}]$. The modeling of diffusion processes requires specification of boundary conditions, the lower one involving drag coefficients; all set to 1.0×10^{-3}. Inclusion of PBL diffusion precludes the need for low-level Rayleigh dissipation but not Newtonian damping of temperature; damping coefficient is $(15\text{ days})^{-1}$ when $\sigma<0.5$, increasing linearly to $(5\text{ days})^{-1}$ at the surface. The momentum and thermodynamic equations also include horizontal diffusive mixing, with a constant coefficient of $5\times10^5\ m^2s^{-1}$. The diffusive and Newtonian damping of temperature occur on isobaric surfaces in the model.

The diagnostic model is solved numerically, using the semi-spectral representation for horizontal structure: 73 grid points between the two poles ($\Delta\theta=2.5°$), and zonal Fourier truncation at wave number 30. The vertical structure is discretized using 18 full-sigma levels of

which 14 are in the troposphere, including 5 below 850 hPa.

Forcing data sets

The zonal-mean zonal and meridional winds, temperature, and surface pressure from ERA-40's 1979-2001 climatology constitute the model's basic state, while orography, 3D diabatic heating and submonthly transient heat and momentum fluxes (diagnosed from 6-hourly reanalyses), and surface temperature from the same data set provide the model forcing. Heating was diagnosed in-house from ERA-40's 23-level and 2.5º resolution isobaric reanalyses (Chan and Nigam 2008). The heating was diagnosed as a residual in the thermodynamic equation (e.g., Hoskins et al. 1989, Nigam 1994) using monthly data and submonthly transient fluxes, just as it was earlier for NCEP and ERA-15 reanalyses in Nigam et al. (2000).

Diagnosed forcing fields are displayed in Fig. 8 to demarcate the regions whose response is analyzed next and for reassurance. The mass-weighted heating average (surface-to-125 hPa) in winter and summer is shown in panels *a*-*b*. Well known features such as the ITCZ, South Pacific Convergence Zone (SPCZ), Maritime Continent convection, Asian monsoon, midlatitude winter stormtracks, and the eastern subtropical Pacific descent and cooling zones are all in evidence; including their seasonal variation. The ERA-40 heating over the Maritime Continent and Pacific and Atlantic ITCZs is substantially stronger than NCEP's, by as much as a factor of 2 (Chan and Nigam 2008). Three regions are outlined on the heating distributions: Asian monsoon, ITCZ+SPCZ, and the Pacific stormtracks.

The storm track region is, in fact, based on the distribution of the 850 hPa meridional wind variance (panels *c*-*d*), which is a commonly used to monitor stormtrack activity (e.g., Chang 1993). Winter variance is largest in the central North Pacific and Atlantic basins, with stormtrack diabatic heating concentrated to the west of the wind variance maximum.

Model performance

A prerequisite for dynamical diagnosis is the diagnostic model's ability to simulate the target field: seasonal SLP *development*, here. If notable development features can be simulated, their origin can be investigated, at least, in a diagnostic (*a posteriori*) sense. For a meaningful analysis, the model should be required to simulate the individual seasonal circulations as well.[13] The model's performance is assessed in Figs. 9-10. In the interest of space, and in order to cover both lower and upper tropospheric circulations, the individual season simulations are assessed using the 200 hPa streamfunction (Fig. 9), while simulation of seasonal *development* (the winter to summer change, i.e., JJA-DJF) is evaluated using SLP (for obvious reasons) in Fig. 10.

The simulated and observed streamfunction (upper panels) compare favorably in amplitude and features, with the possible exception of the Eastern Hemisphere trough-ridge system which is placed ~20° upstream in the simulation and the weaker ridge over northeast Pacific. The summer streamfunctions (lower panels) are also in good agreement but the Tibetan anticyclone is a bit stronger and the Pacific mid-basin trough marginally weaker but more expansive in the simulation. The individual seasonal simulations are, over all, quite realistic.

The difference of the winter and summer SLP simulation is shown in Fig. 10b, while the related ERA-40 target is in panel *a*.[14] An intercomparion shows SLP development to be reasonably simulated, with feature-to-feature correspondence with observations. Deficiencies include a coastal focus and weaker amplitudes in the Pacific basin (by ~4 hPa). The deficiencies are somewhat more pronounced than those manifest in upper-level simulation but, not

[13] Or better yet, their average. The development (*b*−*a*) and average (*b*+*a)* are independent states, and a model that simulates both offers prospects for insightful analysis.

[14] The full fields (zonal-mean + zonal varying) are subtracted in these panels to avoid differences in below-ground interpolation schemes from influencing SLP over the open oceans.

surprisingly, so. The simulation of SLP is challenging given the influence of PBL processes and the difficulties in parameterizing the same. [For this reason, SLP is seldom displayed in diagnostic modeling analyses; low-level streamfunction is, often, shown instead.] The diagnostic model's inability to represent the blocking of flow by orography on account of linearized dynamics further contributes to this challenge.

The fidelity of the individual season simulations and the largely acceptable simulation of winter-to-summer SLP development suggests that the diagnostic model meets the prerequisites for conducting a meaningful dynamical diagnosis of SLP development.

The analysis begins by displaying the response of the winter-to-summer change in diabatic heating and transient fluxes in Fig. 10c.[15] The SLP response is focused in the extratropical basins (~8 hPa), with the longitudinal position of the Pacific maximum in better accord with observations (panel *a*). The Atlantic development is also more realistic. The response forced by heating and transients is of more interest than the full solution as the latter contains a component forced by the surface temperature boundary condition. The boundary condition is introduced in the model from vertical temperature diffusion in the PBL. The related model response is considered part of the local feedback as SSTs underneath the SLP anticyclone are not independent of the overlying circulation.

8. Dynamical diagnoses of winter-to-summer SLP development

Atmospheric diabatic heating and transient fluxes account for a substantial portion of the winter-to-summer SLP development in the extratropical Pacific (cf. Fig. 10c). The geographic regions that most influence this seasonal development are identified in this section from

[15] The solution forced by orography and surface temperature is first subtracted from the full solution for each season, leading to the component forced by heating and transients alone. The winter-to-summer change in this component is shown in Fig. 10c.

diagnostic modeling, with the model's linearity as the basis for the analysis. The forcing regions are marked by rectangles in Fig. 11 which also displays their contribution to SLP development.

The change in forcing over the Asian continent (70-120E, 10-35N), principally from summer monsoon development, enhances SLP over the subtropical Pacific (and Atlantic) by 2-3 hPa, as shown in panel *a*. The response is similar to that arising from just summertime forcing but the winter response (~1 hPa) is not insignificant (both not shown). The impact of Asian continent on Pacific SLP development is modest though, given the 2-3 hPa response vis-à-vis the ~8 hPa signal being diagnosed (Fig. 10c). Rodwell and Hoskins (2001) assessed the influence of the summer monsoon using an expansive forcing region that includes portions of the Western Pacific Warm Pool to the south and the Western North Pacific monsoon to the east (see footnote 9). [Even if relevant in summer, such an expansive region will include both tropical and midlatitude phenomena in winter, compromising its suitability in analysis of SLP development.]

Sea-level pressure development attributable to seasonal change in the tropical Pacific [120E-80W, 17.5S-17.5N] forcing is shown in panel *b*. Heating is dominant in the chosen domain (cf. Fig. 8) which fully captures the ITCZ+SPCZ heating in both winter and summer. The SLP development in the subtropics and midlatitudes is substantial (4-6 hPa), and interestingly, quite similar to the winter response forced from the same region except for sign (not shown), indicating strong influence of the abatement of winter tropical forcing on SLP development.[16] Forcing from the tropical Pacific however provides an incomplete account of SLP development as the related response includes low pressure along the North American coast where the response of global heating and transients is strongly positive (Fig. 10c).

[16] Tropical forcing in summer is much less influential in the model because it is well embedded in the zonal-mean tropical easterlies (about which the model is linearized). Zonal-mean easterlies occur in winter too but in a much narrower equatorial belt (especially in NH), allowing winter forcing to be influential.

Response forced by the change in heating and transients in the Pacific midlatitudes is shown in panel *c*. Both stormtrack heating and transients in winter and low-level diabatic cooling in summer contribute to the forcing change. The resulting response is impressive in the central and eastern midlatitude basin. Regardless of the relative roles of winter stormtrack abatement and summer radiational cooling, the winter-to-summer change in midlatitude forcing can evidently account for much of the SLP development in the central and eastern basin; i.e., for anticyclone build-up. The SLP development generated by the three forcing regions together, i.e., sum of panels *a*-*c*, is shown in panel *d*; which compares favorably with the SLP change shown in Fig. 10c, the target for this dynamical diagnosis. The reconstruction attests to the consideration of the key forcing regions in the diagnosis.

The last panel in Fig. 11 depicts the response of winter heating and transients in the Pacific midlatitudes; it is multiplied by −1 to facilitate comparison with the SLP development (JJA−DJF) plots. The abatement of winter stormtracks generates a response (panel *e*) broadly similar to that forced by the winter-to-summer change in heating and transients (panel *c*). The modest *e*-*c* panel differences in the subtropics and higher latitudes are indicative of the contribution of summer radiational cooling (from stratus cloud-tops in the central and eastern basin) to SLP development.

The role of heating over the North American continent in Pacific SLP development was also assessed, following indications of its importance (Hoskins 1996, Liu et al. 2004, and Miyasaka and Nakamura 2005). The winter-to-summer change in heating and transients over the North American continent (120-75W, 20-60N) generated weak SLP development over the Pacific extratropics (not shown), at least, in our analysis. The SLP response was of the right sign (+) but of weak amplitude (~1 hPa). The response was somewhat more consequential along the Baja Coast where it lowers SLP.

9. Concluding Remarks

The study seeks to advance understanding of the causes of seasonal SLP variability over the NH ocean basins, in particular, the waxing and waning of the Pacific anticyclone – a majestic feature, occupying almost the entire extratropical basin in July. Because of its expanse, perhaps, the Pacific anticyclone has not acquired a different name, unlike its Atlantic counterpart, which is known as the Azores (or Bermuda) High. Sea-level pressure is, of course, one of the most analyzed meteorological variables (e.g., Walker and Bliss 1932) but its seasonal variability, as reflected in the summer strength and expanse of the NH anticyclones, has defied understanding because of the timing, which is counterintuitive from the Hadley Cell perspective.

A number of studies have sought understanding of this counterintuitive evolution since the paradox was eloquently posed by Hoskins (1996). Given the summer vigor of the NH anticyclones, monsoons were implicated. Diagnostic modeling of the summer circulation (e.g., Ting 1994, Rodwell and Hoskins 2001) did show monsoon latent heating to the east and the west of the anticyclone to be important for the summer structure, in addition to local low-level diabatic cooling (of radiative origin) which is more feedback than causative in nature. Given these dynamical analyses which are quite robust, one may well ask why the origin of anticyclone seasonality is being revisited in this paper.

The motivation for revisiting the paradoxical evolution of the Pacific anticyclone came from analysis of seasonal SLP variability, especially the structure and magnitude of SLP *change* over two-month periods, beginning January (Fig. 3). This straightforward analysis shows the

- Winter-to-summer SLP change to be *gradual*, consisting of three comparable 2-month changes. Anticyclone build-up leading to the majestic summer structure is thus not

confined to the monsoon-onset period (May-July). Waxing and waning of the anticyclone must therefore be due to more than just the onset and demise of the summer monsoons.

- In the build-up phase, positive SLP development is focused in the extratropical basin (northward of the Tropic of Cancer). The tropical-subtropical basin exhibits modest SLP change, 1-2 hPa, with the monsoon-onset period change being, in fact, negative!
- Tracking anticyclone's evolution via the 1020 hPa isobar in the full SLP field (physically appealing) confirms that SLP change in the tropical and subtropical basin is quite modest

The evolution of other prominent anticyclones – Azores (Bermuda) High in the NH and the Mascarene High in the SH – was also examined with the hope that intercomparisons may shed light on the development mechanisms. We found the Azores High and Pacific anticyclone evolutions to be similar, both exhibiting peak amplitude/expanse in summer. Annual SLP variability in the Atlantic also exhibits largest amplitudes in the high latitudes and modest variability in the subtropics. The similarity, despite the absence of an Asian monsoon equivalent to the west, suggests that either a monsoon to the west is inconsequential, the global reach of the Asian monsoon, and/or the significant influence of stormtrack abatement in each basin.

The SH anticyclones are found to peak in austral winter, in contrast with the northern ones. This peak-phase timing rules out SH monsoons and stormtracks as causative influence; the latter, not surprising, given their sub-polar, distant location. Waxing and waning of the SH anticyclones can be accounted for by Hadley Cell's seasonality – in accordance with dynamical intuition that proved incorrect in the NH (due to interference from robust stormtrack and monsoon influences).

If monsoons cannot be implicated in the summer vigor of the Pacific anticyclone, the paradox that Hoskins posed stands. The paradox is resolved by first noting that it is the weak seasonality of SLP in the tropics-subtropics (Figs. 2-4) rather than perceptions of a large

counterintuitive (i.e., positive) signal there (cf. Hoskins 1996) that is perplexing in context of the striking winter-to-summer weakening of the Hadley Cell. [Positive SLP development does occur in summer but well to the north (~45N), as shown in Figs. 2-4.] The striking seasonality of the Hadley Cell is, moreover, shown to arise from (and thus represent) descent variations related to Asian summer monsoon onset and demise; consistent wth Dima and Wallace (2003). Descent over the central-eastern basins (anticyclone domain), in fact, exhibits far less seasonal variation than implied by Hadley Cell's striking seasonality along with flawed notions of it being zonally representative; resolving the paradox.

The apparent contradiction between observational findings and modeling analyses on the role of monsoons in anticyclone development arises not because either is flawed, but because the two cannot be directly compared: Modeling studies have hitherto targeted the summer circulation itself, not circulation development (cf. Fig. 3), the pertinent target in context of the summer peaking of anticyclone's strength/expanse. Anticyclone development, especially when gradual, can depend as much on forcing onsets as abatements. This suggests that mechanisms posited for the summer robustness of the NH anticyclones from modeling analyses need to be reaffirmed.

Dynamical diagnosis of circulation development over the Pacific concludes this inquiry. A steady, linear primitive equation model that reasonably simulates winter-to-summer (JJA−DJF) SLP development when forced by ERA-40 derived diabatic heating and transient fluxes is used to assess the contributions of three forcing regions: Asian monsoon, Pacific Tropics, and the Pacific midlatitudes. Of the three, Pacific midlatitudes is most influential, contributing, at least, two-thirds of the SLP development signal (6-8 hPa), with the bulk coming from the abatement of winter stormtrack heating and transients. The Asian monsoon contribution (2-3 hPa) is dominant in the Pacific (and Atlantic) tropics-subtropics. The response of Pacific ITCZ+SPCZ heating is

confined to the western and far eastern extratropical basin, with the former being influential.

The diagnostic (*a posteriori*) nature of the modeling assessment and the employed model's simplicity and potential weaknesses (e.g., linearization about a zonal-mean basic state, PBL treatment, etc.) necessitate corroboration of the modeling analysis. For instance, Rodwell and Hoskins (2001) find the blocking of flow by mountain ranges to be important for anticyclone development in the eastern basins, but this effect is not modeled by the linearized dynamics used in this study. On the other hand, the modeling results resonate with the observational findings reported in the first part of the paper.

Acknowledgements

We wish to thank Brian Hoskins and an anonymous reviewer for reading our manuscript and for their constructive suggestions, and Editor Clara Deser for guidance. Sumant Nigam acknowledges NOAA and NSF support through CPPANA17EC1483 and ATM-0649666 grants. Steven Chan was supported by the NASA Earth System Science Fellowship (2004-2007).

References

Bergeron, T., 1930: Richlinien einer dynamischen klimatologie. *Met. Zeit.,* **47,** 246-262.

Bjerknes, J., 1935: La circulation atmosphérique dans les latitudes sous-tropicales. *Scientia,* **57,** 114-123.

Chan, S. C., and S. Nigam, 2008: Residual diagnosis of diabatic heating from ERA-40 and NCEP reanalyses: Intercomparisons with TRMM . *J. Climate* (in press)

Chang, E. K. M., 1993: Downstream development of baroclinic waves as inferred from regression analysis. *J. Atmos. Sci.*, **50**, 2038-2053.

Chen, P., M. P. Hoerling, and R. M. Dole, 2001: The origin of the subtropical anticyclone. *J. Atmos. Sci.,* **58,** 1827-1835.

Dima, I. M., and J. M. Wallace, 2003: On the seasonality of the Hadley Cell. *J. Atmos. Sci.,* **60,** 1522-1527.

Held, I. M., S. W. Lyons, and S. Nigam, 1989: Transients and the extratropical response to El Nino. *J. Atmos. Sci.,* **46,** 163-174.

Hoskins, B. J., 1996: On the existence and strength of the summer subtropical anti-cyclones. *Bull. Amer. Meteor. Soc.,* **77,** 1287-1291.

_____, B. J., and P. J. Valdes, 1990: On the existence of storm-tracks. *J. Atmos. Sci.,* **47,** 1854-1864.

_____, and_____, 2002: New perspectives on Northern Hemisphere winter storm tracks. *J. Atmos. Sci.,* **59,** 1041-1061.

_____, and_____, 2005: A new perspective on S. Hemisphere storm tracks. *J. Climate,* **18,** 4108-4129.

_____, et al. 1989: Diagnostics of the global atmospheric circulation based on ECMWF analyses 1979-1989. WCRP-27; WMO/TD-No. 326, *217pp*.

Kållberg, P., P. Berrisford, B. J. Hoskins, A. Simmons, S. Uppala, S. Lamy-Thépaut, and R. Hine, 2005: *ERA-40 Atlas.* ERA-40 Project Report Series. No.19, ECMWF, 103 pp.

Karoly, D. J., and B. J. Hoskins, 1982: Three dimensional propagation of planetary wave. *J. Meteor. Soc. Japan.,* **60**, 109-123,

Krishnamurti, T. N., and H. N. Bhalme, 1976: Oscillations of a monsoon system. Part I. Observational aspects. *J. Atmos. Sci.,* **33,** 1937-1954.

Liu, Y., G. Wu, and R. Ren, 2004: Relationship between the subtropical anticyclone and diabatic heating. *J. Climate,* **17,** 682-698.

Miyasaka, T., and H. Nakamura, 2005: Structure and formation mechanisms of the northern hemisphere summertime subtropical highs. *J. Climate,* **18,** 5046-5065.

Newell, R. E., J. W. Kidson, D. G. Vincent, and G. J. Boer, 1972: *The General Circulation of the Tropical Atmosphere and Interactions with Extratropical Latitudes,* Vol. 1. MIT Press, 258 pp.

Nigam, S., 1997: The annual warm to cold phase transition in eastern equatorial Pacific: Diagnosis of the role of stratus cloud-top cooling. *J. Climate,* **10,** 2447-2467.

_____, and R. S. Lindzen, 1989: The sensitivity of stationary waves to variations in the basic state zone flow. *J. Atmos. Sci.,* **12,** 1746-1768.

_____, 1994: On the dynamical basis for the Asian summer monsoon rainfall – El Niño relationship. *J. Climate,* **7,** 1750-1771.

_____, C. Chung, and E. DeWeaver, 2000: ENSO diabatic heating in ECMWF and NCEP reanalyses, and NCAR CCM3 simulation. *J. Climate,* **13,** 3152-3171.

_____, and A. Ruiz-Barradas, 2006: Seasonal hydroclimate variability over North America in global and regional reanalyses and AMIP simulations: Varied representation. *J. Climate,* **19,** 815-837.

Peterson, M., 2005: *Naming the Pacific.* Vol. 5, No. 2, January 2005. http://www.common-place.org/vol-05/no-02/peterson/index.shtml

Petterssen, S., 1940: *Weather analysis and forecasting*. McGraw-Hill, 505 pp.

Pierrehumbert, R. T., 1995: Thermostats, radiator fins, and local runaway greenhouse. *J. Atmos. Sci.,* **52,** 1784-1806.

Rodwell, M. J., and B. J. Hoskins, 1996: Monsoons and the dynamics of deserts. *Quart. J. Roy. Meteor. Soc.,* **122,** 1385-1404.

_____, and _____, 2001: Subtropical anticyclones and summer monsoons. *J. Climate,* **14,** 3192-3211.

Sardeshmukh, P. D., 1993: The baroclinic χ problem and its application to the diagnosis of atmospheric heating rates. *J. Atmos. Sci*., **50**, 1099-1112

Seager, R., R. Murtugudde, A. Clement, A. Gordon, and R. Miller, 2003: Air-sea interaction and the seasonal cycle of the subtropical anticyclones. *J. Climate,* **16,** 1948-1965.

Ting, M., 1994: Maintenance of northern summer stationary waves in a GCM. *J. Atmos. Sci.,* **51,** 3286-3308.

Uppala, S., and Coauthors, 2005: The ERA-40 Re-analysis. *Quart. J. Roy. Meteor. Soc.,* **131,** 2961-3012.

Walker, G. T. and E. W. Bliss, 1932: World weather V. *Mem. Roy. Meteorol. Soc.*, **4**, 53-84.

Xie, P., and P.A. Arkin, 1997: Global precipitation: A 17-year monthly analysis based on gauge observations, satellite estimates, and numerical model outputs. *Bull. Amer. Meteor. Soc.,* **78,** 2539-58.

Figure Captions

1. Cold-to-warm season evolution of sea-level pressure (contoured) and precipitation (shaded) in the 1979-2001 period monthly climatology. SLP is from ERA-40 and precipitation from CMAP-2: (a) January, (b) March, (c) May, and (d) July. SLP is contoured every 3.0 hPa, and precipitation shaded at 4.0 mm/day intervals, beginning at 4.0 mm/day, as indicated by the color bar. Major SLP centers – Pacific High and the Aleutian Low – are marked. The Tropic of Cancer (drawn) provides positional reference during seasonal evolution.

2. Monthly evolution of the Pacific High – the sea-level pressure anticyclone in the Northern Hemisphere. The 1020 hPa isobar in the climatological (1979-2001) SLP field is tracked at two-month intervals, beginning January. Isobars are labeled by the calendar month number; for example, January is '1' and November '11'. The cold-to-warm season development essentially consists of a westward and northward expansion of the anticyclone.

3. Pacific **s**ea-level pressure *development*: The two-month change in climatological SLP. (a) January to March, (b) March to May, (c) May to July, (d) July to September, (e) September to November, and (f) November to January. The SLP change is contoured at 1.0 hPa interval, with solid (dashed) contours indicating positive (negative) development. The Tropic of Cancer is again shown for positional reference.

4. Annual-mean and annual-cycle of sea-level pressure in the Pacific and Atlantic basins, based on ERA-40 monthly climatology (1979-2001). Annual-mean SLP is contoured at 2.0 hPa intervals, with values above (below) 1018 (1010) hPa shaded. The annual variability is displayed using vectors, with the length denoting amplitude, and the direction, the phase; as indicated

above. A *locally* northward pointing vector, for example, indicates maximum (minimum) SLP in July (January). Vectors are not drawn when the variability amplitude is less than 0.5 hPa.

5. Monthly evolution of the 300 hPa vertical velocity ($-\omega_{300}$) in the NH subtropics (15N-25N); based on ERA-40 climatology (1979-2001). Longitudinal distribution is shown in the left panel while evolution of the corresponding zonal-mean is in the right one. Contour interval is 0.5 hPa/hour and the zero-contour omitted.

6. Divergent circulation in the upper troposphere in June-August (upper panel) and December-February (lower panel), based on ERA-40 climatology (1979-2001). The 200 hPa divergence is contoured at 10^{-6} s^{-1} intervals and the divergent wind vector is displayed using the indicated scale. Solid (dashed) contours indicate positive (negative) divergence, and the zero-contour is omitted.

7. Annual-mean and annual-cycle of sea-level pressure in the global Southern Hemisphere, based on ERA-40 monthly climatology (1979-2001). A *locally* northward pointing vector, for example, indicates maximum SLP in July, as before. Rest as in Figure 4.

8. Vertically-averaged ERA-40 diabatic heating in winter (DJF) and summer (JJA) seasons in the 1979-2001 period climatology is shown in panel *a-b*. Heating is residually diagnosed and the surface-to-125 hPa mass-weighted average is displayed with a 0.75 K/day interval. The submonthly meridional wind variance at 850 hPa, an indication of transient activity, is shown in the corresponding periods in panels *c-d*, with a 15 m^2/s^2 interval. Red (blue) color indicates positive (negative) values and the zero-contour is omitted in all panels. The superposed rectangles outline three forcing regions whose responses are analyzed in a later section: Asian monsoon (70-120E, 10-35N), ITCZ heating (120E-80W, 17.5S-17.5N), and Pacific storm tracks

(135E-130W, 27.5-60N).

9. Diagnostically modeled and observed 200 hPa eddy streamfunction in winter (left) and summer (right) in the 1979-2001 period climatology. The contour interval is 4.0E6 m^2/s, or ~40 gpm in the midlatitudes, and the red (blue) color indicates positive (negative) values. The zero-contour is omitted in all panels.

10. Diagnostically modeled and observed winter-to-summer *development* in sea-level pressure (SLP) in the 1979-2001 period climatology: *a)* ERA-40, *b)* Diagnostic simulation, from the difference of winter and summer solutions, and *c)* Simulation component due to changes in 3D diabatic heating and vorticity and thermal transients, i.e., without lower boundary (orography and surface temperature) influences. The contour interval is 2.0 hPa and the red (blue) color indicates positive (negative) values. The zero-contour is omitted in all panels, as before.

11. Dynamical diagnosis of the linearly simulated winter-to-summer SLP *development* forced by seasonal changes in heating and transients (i.e., of figure 10c): Component forced by the JJA-DJF changes in heating and transients over *a)* Asian monsoon region, *b)* Pacific ITCZ+SPCZ, *c)* Pacific midlatitudes, and *d)* sum of the above. Panel *e* shows SLP forced by winter heating and transients in the Pacific midlatitudes, after multiplication by −1. The contour interval is 2.0 hPa and the red (blue) color indicates positive (negative) values in each panel. Zero-contour is omitted in all panels, as before.

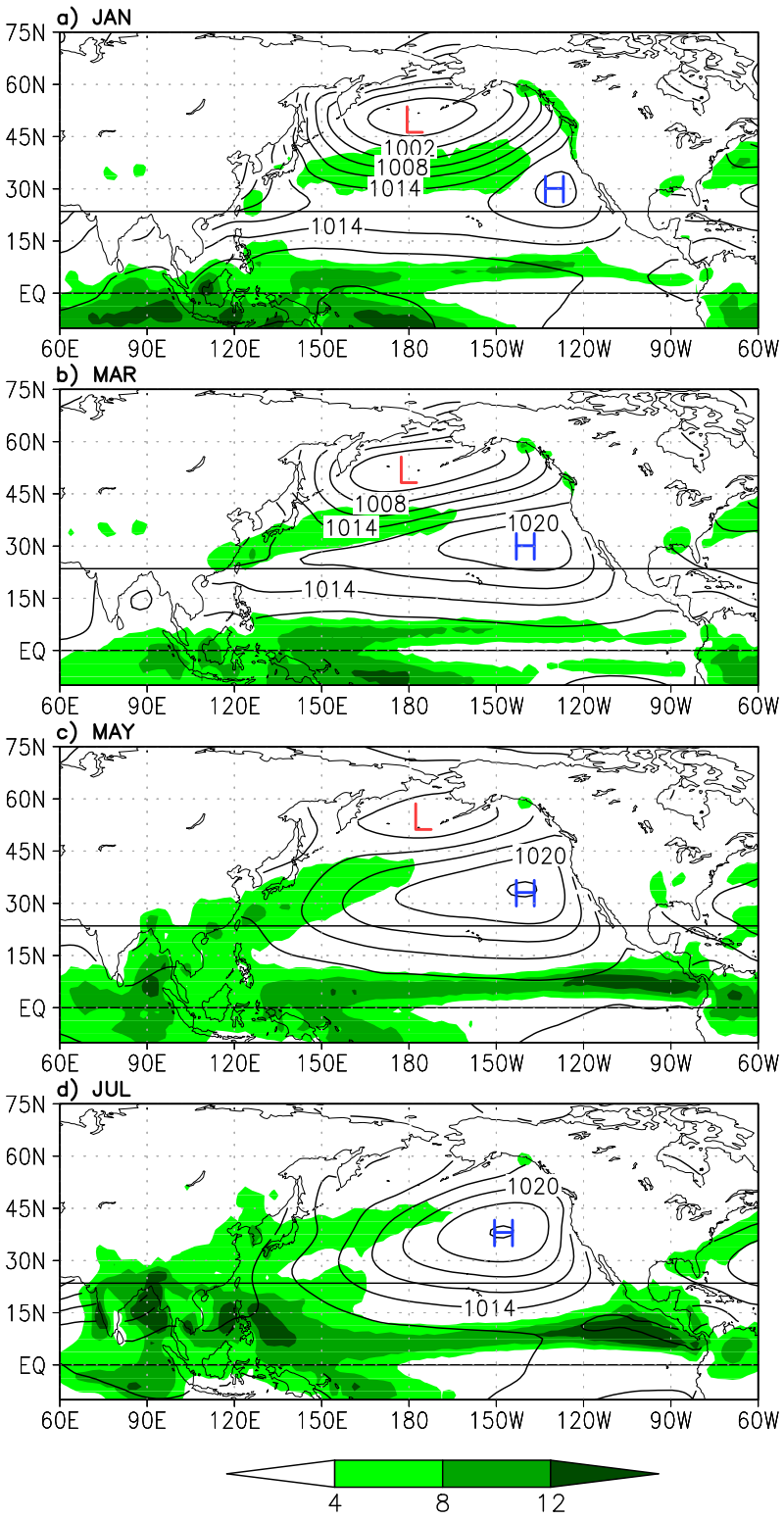

Figure 1: Cold-to-warm season evolution of sea-level pressure (contoured) and precipitation (shaded) in the 1979-2001 period monthly climatology. SLP is from ERA-40 and precipitation from CMAP-2: (a) January, (b) March, (c) May, and (d) July. SLP is contoured every 3.0 hPa, and precipitation shaded at 4.0 mm/day intervals, beginning at 4.0 mm/day, as indicated by the color bar. Major SLP centers – Pacific High and the Aleutian Low – are marked. The Tropic of Cancer (drawn) provides positional reference during seasonal evolution.

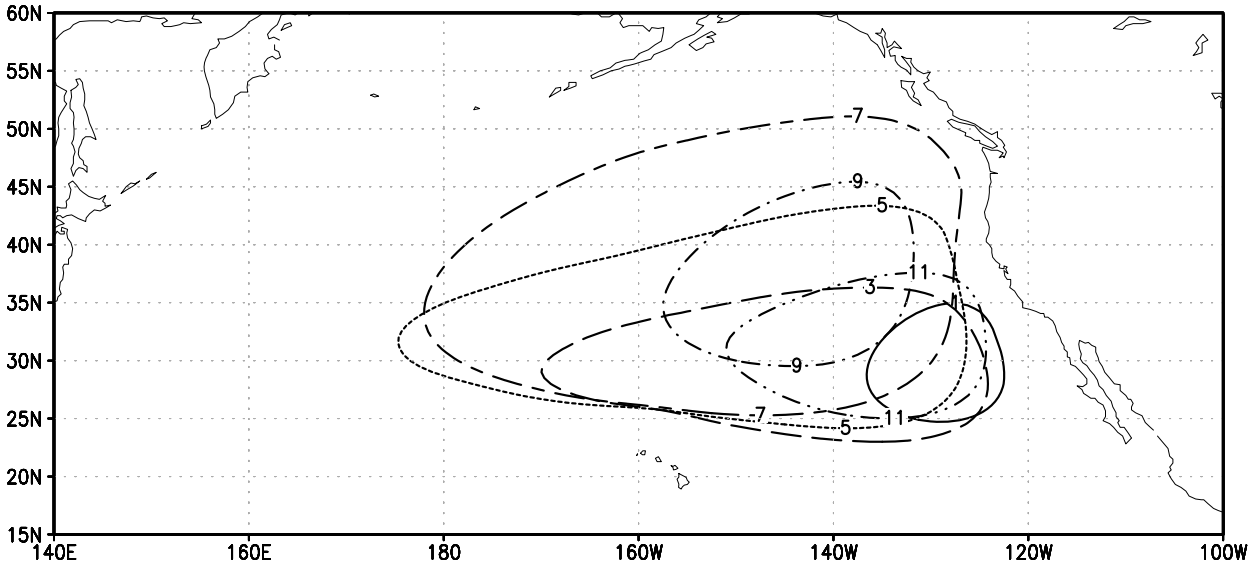

Figure 2: Monthly evolution of the Pacific High – the sea-level pressure anticyclone in the Northern Hemisphere. The 1020 hPa isobar in the climatological (1979-2001) SLP field is tracked at two-month intervals, beginning January. Isobars are labeled by the calendar month number; for example, January is '1' and November '11'. The cold-to-warm season development essentially consists of a westward and northward expansion of the anticyclone.

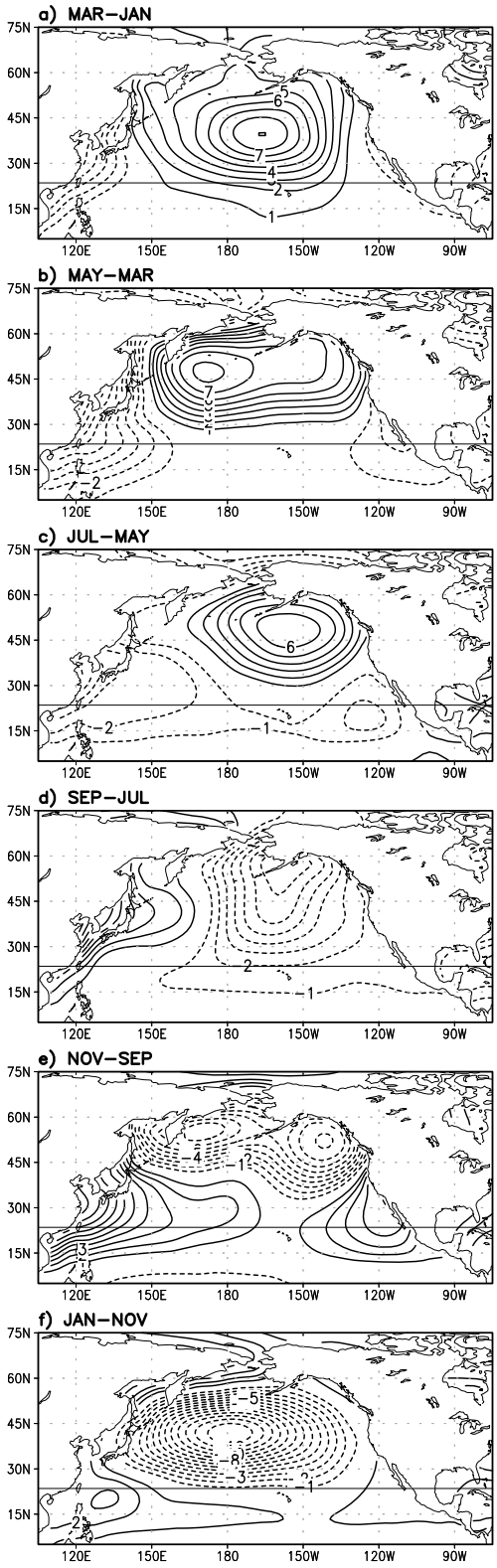

Figure 3: Pacific **s**ea-level pressure *development*: The two-month change in climatological SLP. (a) January to March, (b) March to May, (c) May to July, (d) July to September, (e) September to November, and (f) November to January. The SLP change is contoured at 1.0 hPa interval, with solid (dashed) contours indicating positive (negative) development. The Tropic of Cancer is again shown for positional reference.

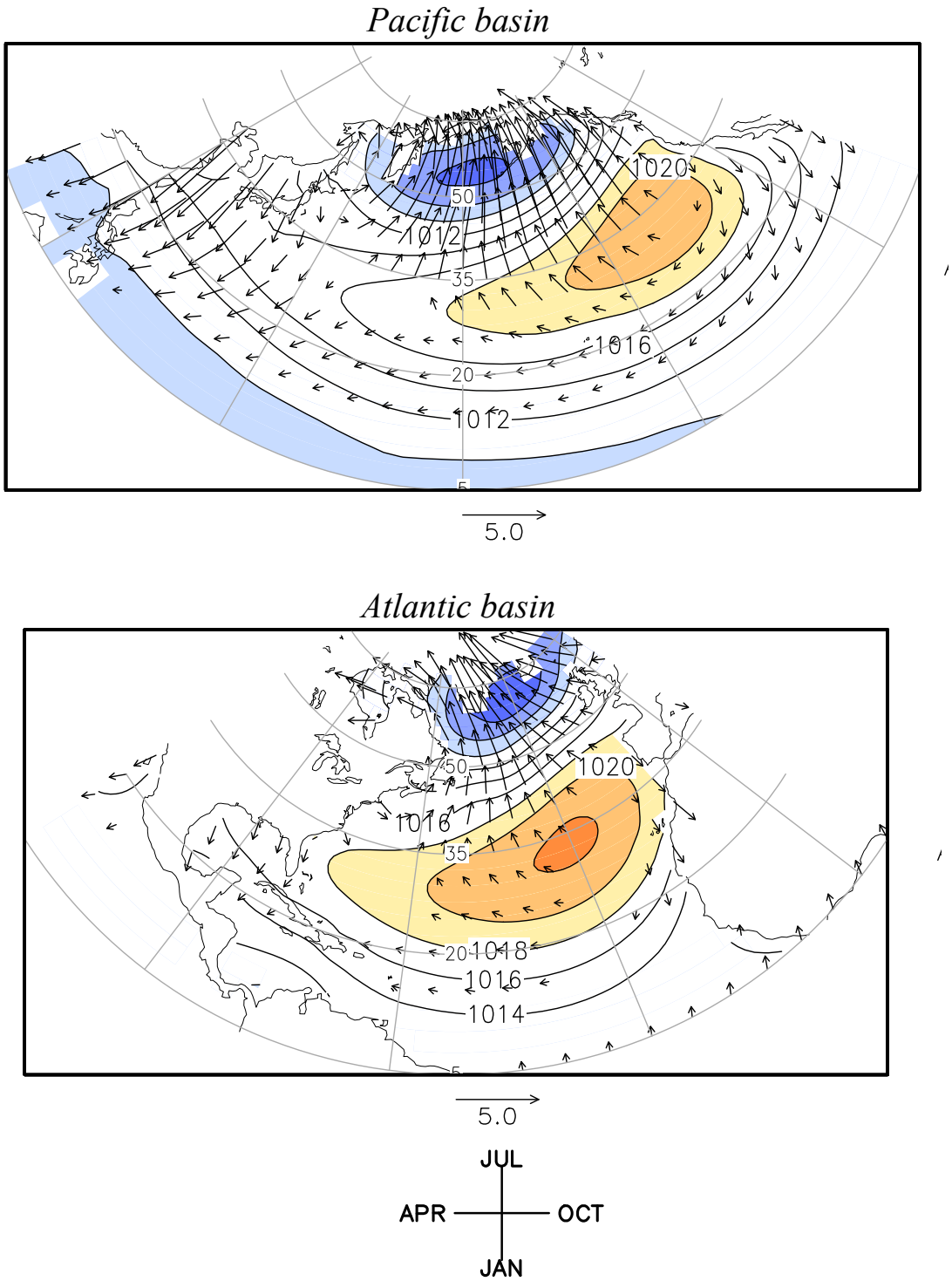

Figure 4: Annual-mean and annual-cycle of sea-level pressure in the Pacific and Atlantic basins, based on ERA-40 monthly climatology (1979-2001). Annual-mean SLP is contoured at 2.0 hPa intervals, with values above (below) 1018 (1010) hPa shaded. The annual variability is displayed using vectors, with the length denoting amplitude, and the direction, the phase; as indicated above. A *locally* northward pointing vector, for example, indicates maximum (minimum) SLP in July (January). Vectors are not drawn when the variability amplitude is less than 0.5 hPa.

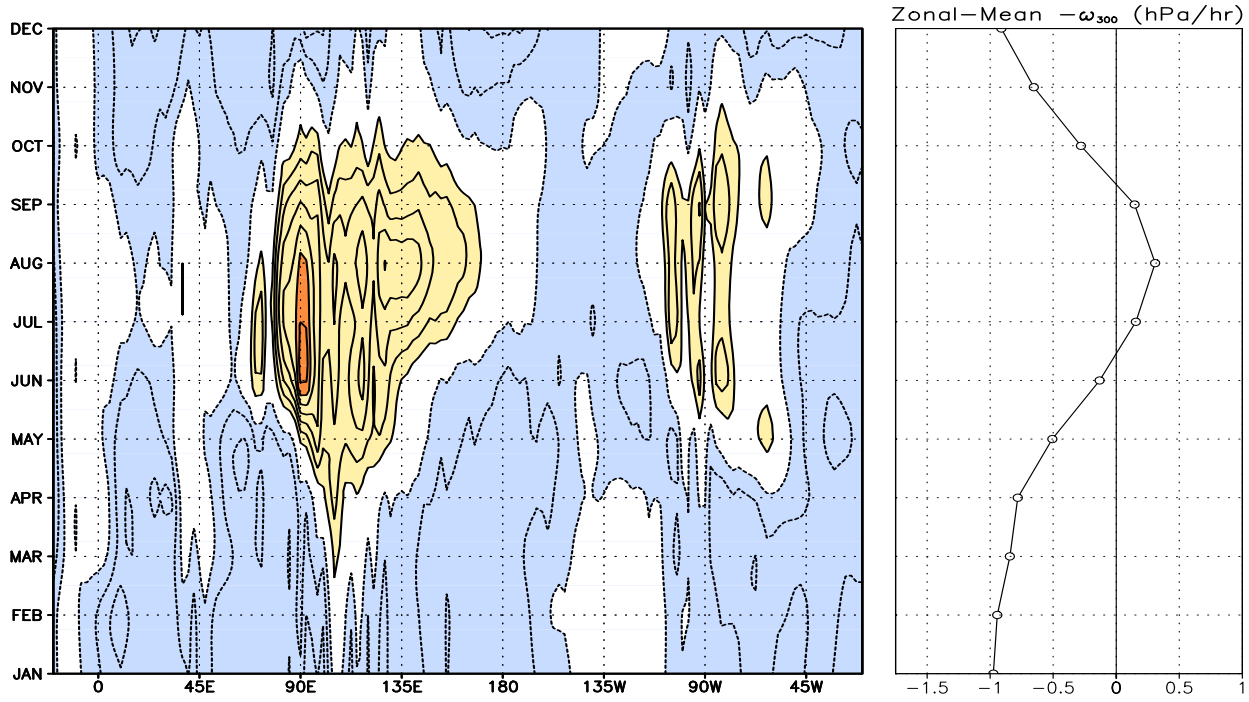

Figure 5: Monthly evolution of the 300 hPa vertical velocity ($-\omega_{300}$) in the NH subtropics (15N-25N); based on ERA-40 climatology (1979-2001). Longitudinal distribution is shown in the left panel while evolution of the corresponding zonal-mean is in the right one. Contour interval is 0.5 hPa/hour and the zero-contour omitted.

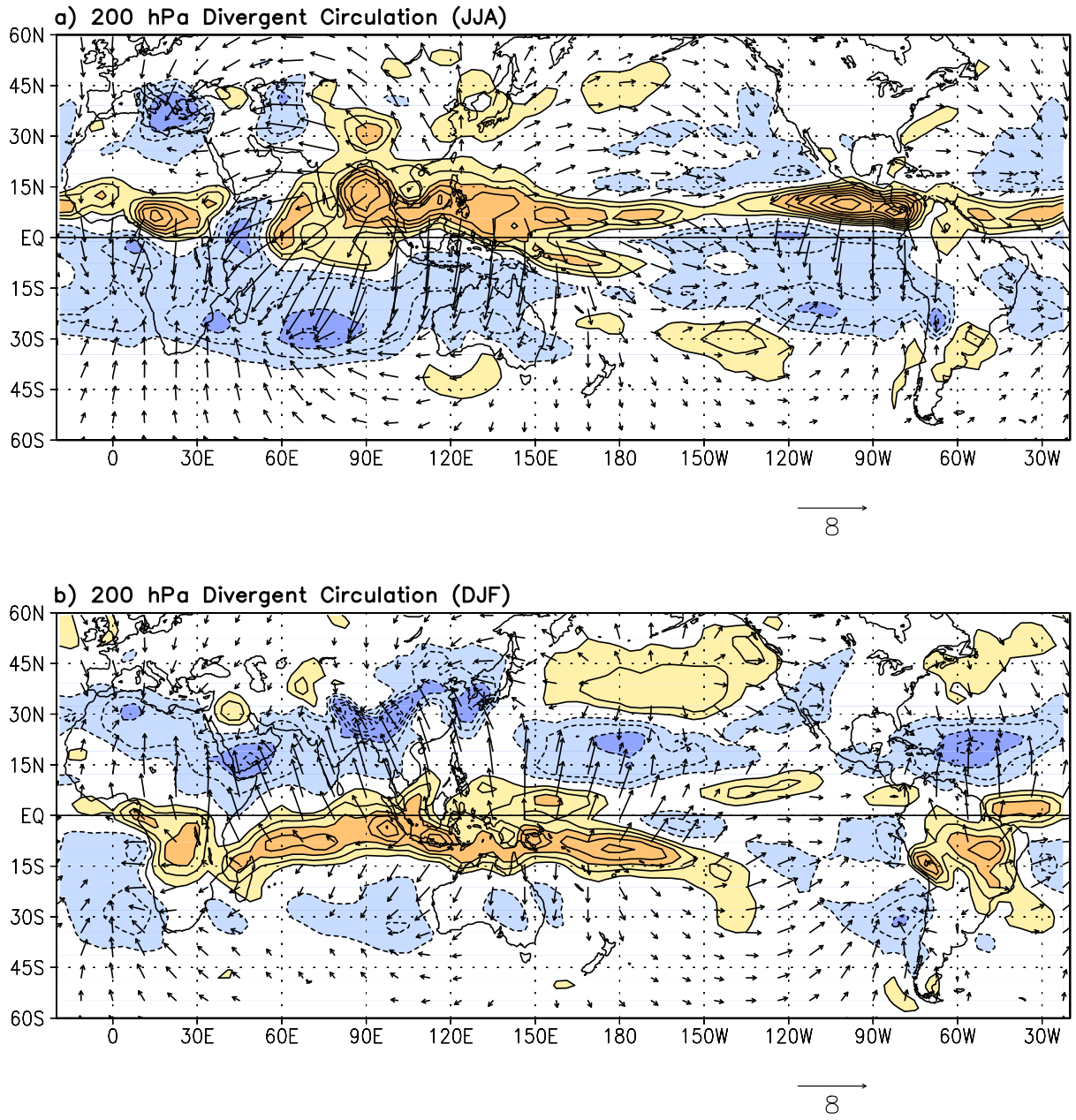

Figure 6: Divergent circulation in the upper troposphere in June-August (upper panel) and December-February (lower panel), based on ERA-40 climatology (1979-2001). The 200 hPa divergence is contoured at 10^{-6} s^{-1} intervals and the divergent wind vector is displayed using the indicated scale. Solid (dashed) contours indicate positive (negative) divergence, and the zero-contour is omitted.

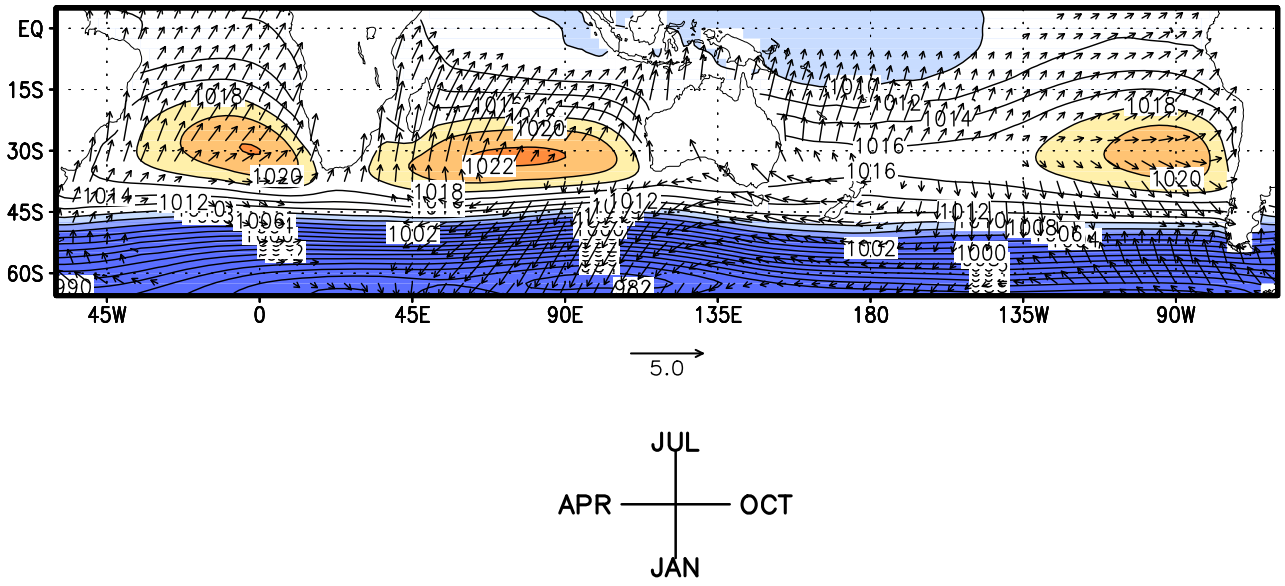

Figure 7: Annual-mean and annual-cycle of sea-level pressure in the global Southern Hemisphere, based on ERA-40 monthly climatology (1979-2001). A *locally* northward pointing vector, for example, indicates maximum SLP in July, as before. Rest as in Figure 4.

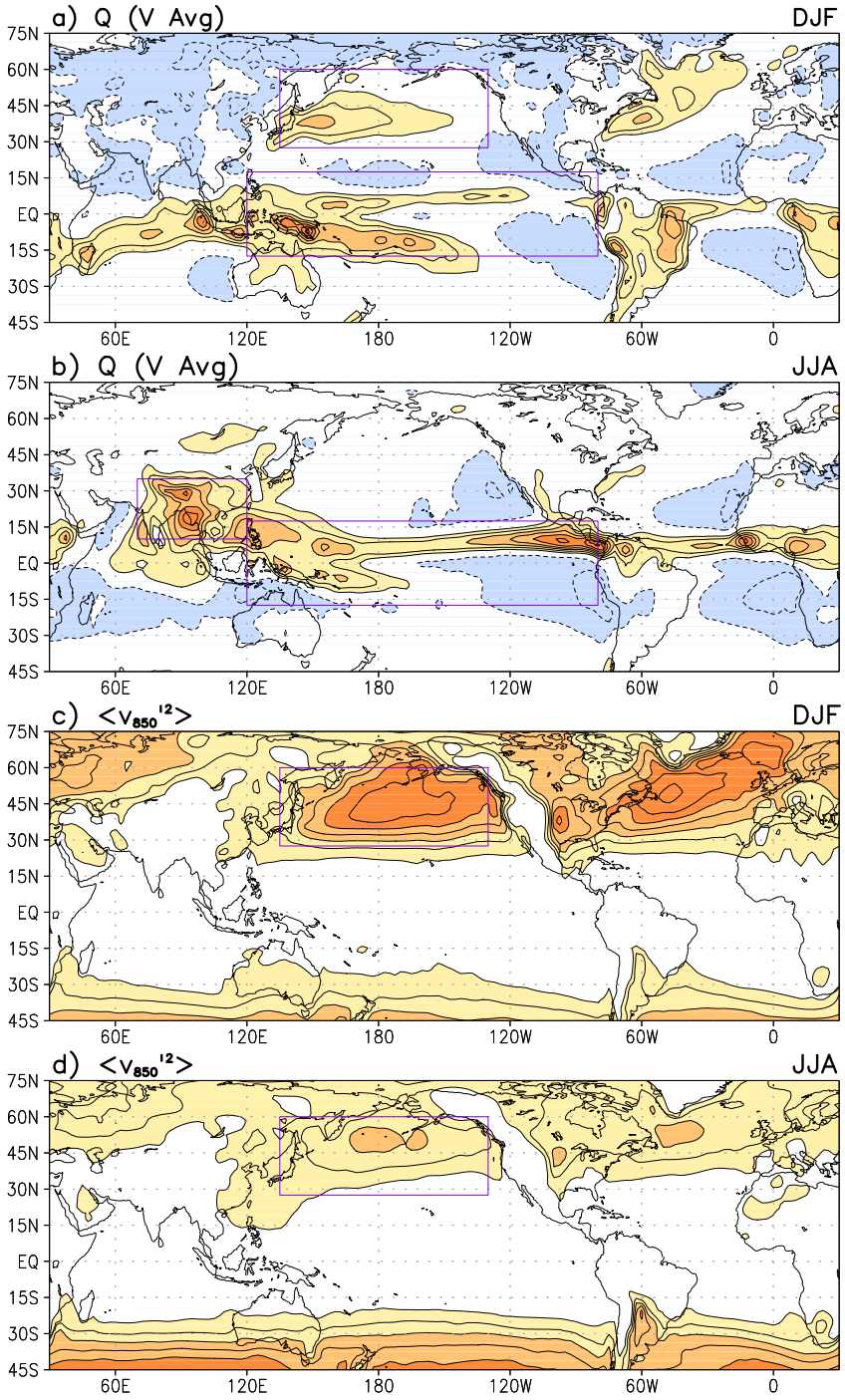

Figure 8: Vertically-averaged ERA-40 diabatic heating in winter (DJF) and summer (JJA) seasons in the 1979-2001 period climatology is shown in panel *a-b*. Heating is residually diagnosed and the surface-to-125 hPa mass-weighted average is displayed with a 0.75 K/day interval. The submonthly meridional wind variance at 850 hPa, an indication of transient activity, is shown in the corresponding periods in panels *c-d*, with a 15 m^2/s^2 interval. Red (blue) color indicates positive (negative) values and the zero-contour is omitted in all panels. The superposed rectangles outline three forcing regions whose responses are analyzed in a later section: Asian monsoon (70-120E, 10-35N), ITCZ heating (120E-80W, 17.5S-17.5N), and Pacific storm tracks (135E-130W, 27.5-60N).

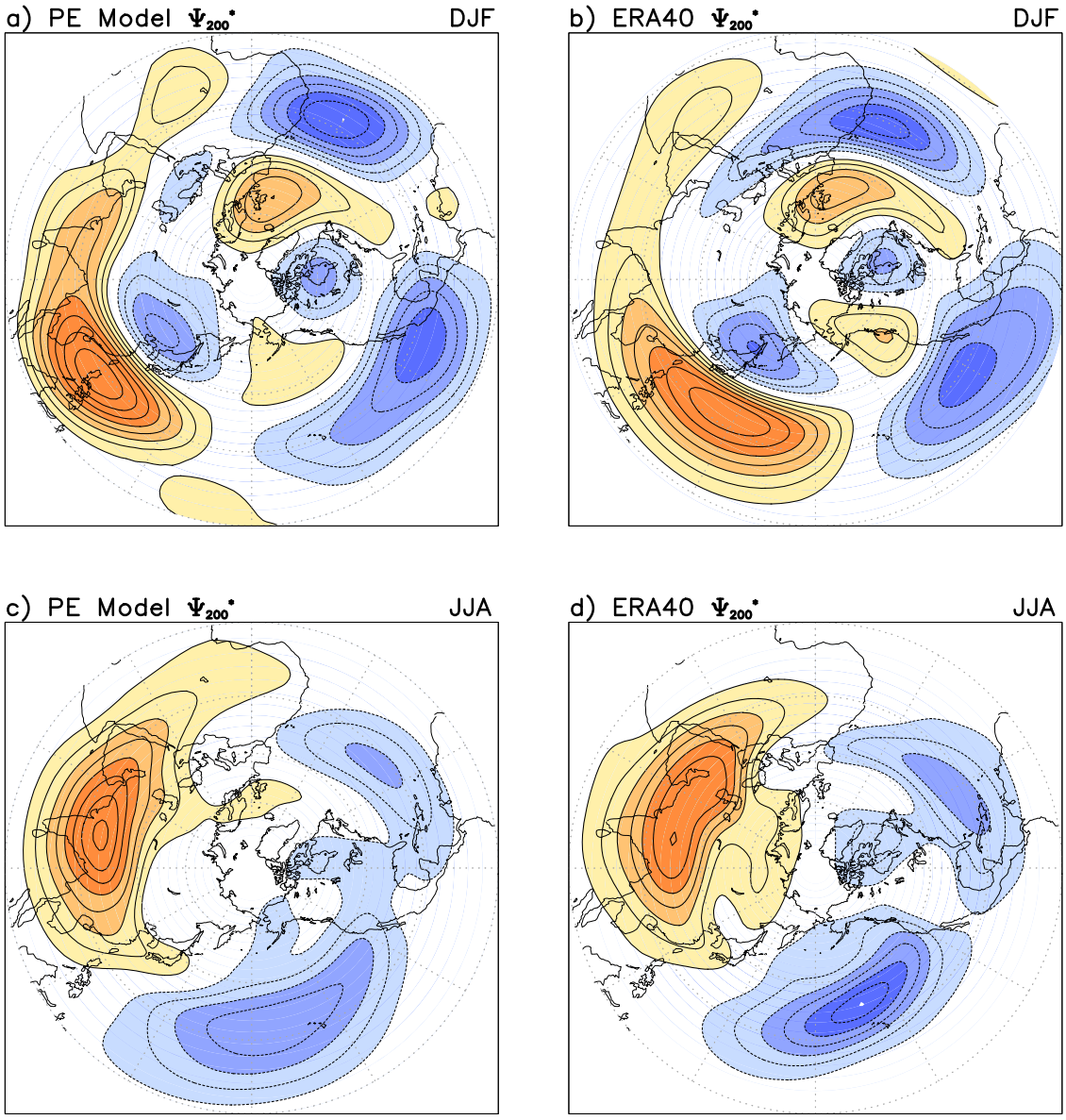

Figure 9: Diagnostically modeled and observed 200 hPa eddy streamfunction in winter (left) and summer (right) in the 1979-2001 period climatology. The contour interval is 4.0E6 m^2/s, or ~40 gpm in the midlatitudes, and the red (blue) color indicates positive (negative) values. The zero-contour is omitted in all panels.

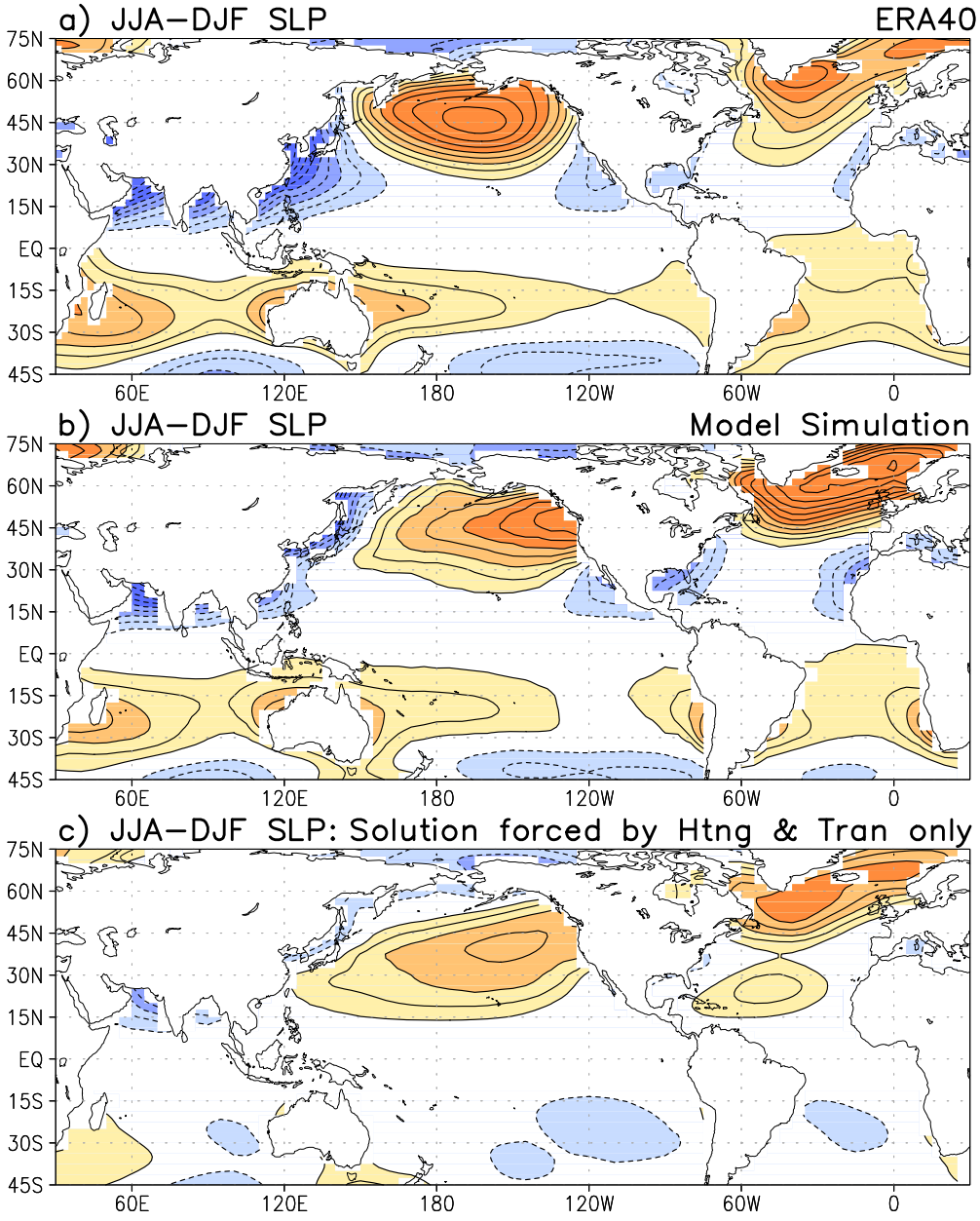

Figure 10: Diagnostically modeled and observed winter-to-summer *development* in sea-level pressure (SLP) in the 1979-2001 period climatology: *a)* ERA-40, *b)* Diagnostic simulation, from the difference of winter and summer solutions, and *c)* Simulation component due to changes in 3D diabatic heating and vorticity and thermal transients, i.e., without lower boundary (orography and surface temperature) influences. The contour interval is 2.0 hPa and the red (blue) color indicates positive (negative) values. The zero-contour is omitted in all panels, as before.

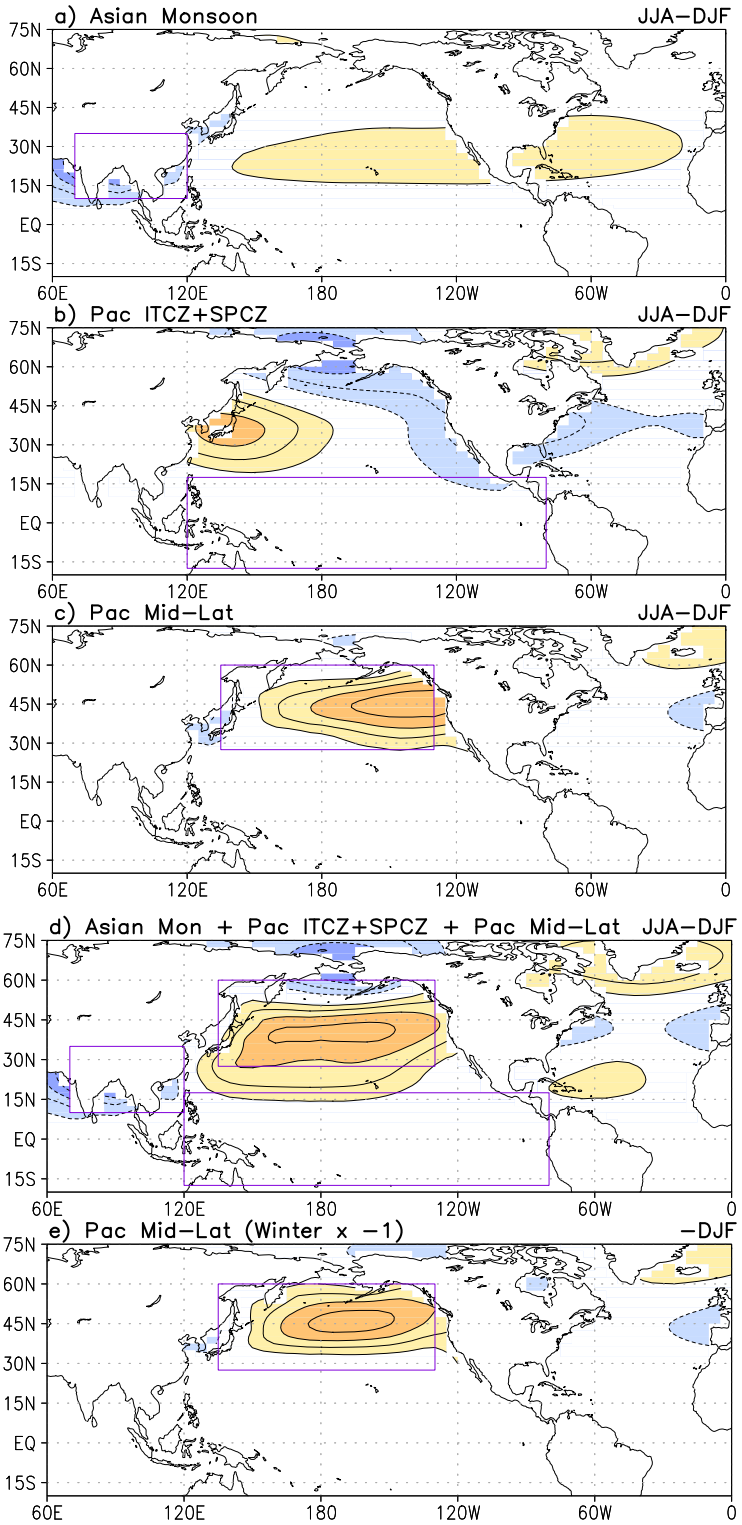

Figure 11: Dynamical diagnosis of the linearly simulated winter-to-summer SLP *development* forced by seasonal changes in heating and transients (i.e., of figure 10c): Component forced by the JJA-DJF changes in heating and transients over *a)* Asian monsoon region, *b)* Pacific ITCZ+SPCZ, *c)* Pacific midlatitudes, and *d)* sum of the above. Panel *e* shows SLP forced by winter heating and transients in the Pacific midlatitudes, after multiplication by −1. The contour interval is 2.0 hPa and the red (blue) color indicates positive (negative) values in each panel. Zero-contour is omitted in all panels, as before.